

# Far-Infrared Spectra of the Alloy of Germanium-Antimony-Tellurium in the Glassy and Crystalline State

## ABSTRACT

Far-infrared spectra of a germanium-antimony-tellurium alloy in the glassy and crystalline states have been measured and analyzed in the frequency range 20–400 cm<sup>-1</sup> at room temperature. The absorption in this range is due to the phonon modes of the structural units of crystalline and correlated librational vibrations (boson peak) of glassy alloy, which precede the appearance of relaxation dynamics. The vibrational assignments of various absorption bands and the differences revealed in the spectra will make it possible to more confidently elucidate the possible molecular mechanism of the crystal-to-amorphous transition in other chalcogenide alloys. New details of the crystal-to-amorphous transition scenario are suggested.

*Keywords: far-infrared spectra, phonons, boson peak, chalcogenide, phase transition.*

## 1. INTRODUCTION

Phase-change materials (PCMs) based on chalcogenide alloys are of great technological importance due to their ability to undergo on being heated a fast and reversible transition between the amorphous and crystalline phases [1, 2]. This property is exploited in rewritable optical media and electronic nonvolatile memory, which are based on the strong optical and electronic contrast between the two phases [3].

Te-containing chalcogenides such as the Ge-Sb-Te ternary alloy system usually abbreviated as GST has been known to satisfy material requirements for PCMs. The system is already in use for the rewritable compact discs and digital versatile discs and their commercial application in electronic non-volatile memory devices is expected in the near future as well. However, neither the local structure of material nor the change in the structure during the phase transition is well established. Several details of the GST electronic structure, supposed to control the transport properties and the switching mechanism, are still a matter of debate. In some reports, the strong optical and electronic contrast between the amorphous and crystalline phases GST system is attributed to a change in the coordination numbers [4], and in others, to a change of bonding upon crystallization [5] or to a

high concentration of defects [6] and Peierls-distortion in an octahedral environment of Ge atoms [7].

At present, the most advanced techniques, such as the extended x-ray absorption fine structure (EXAFS) spectroscopy and spectroscopy of neutron scattering and Raman scattering (RS) are employed in studies of the local atomic structure and dynamics of GST. Interestingly, the infrared (IR) spectroscopy is rarely used [8], and no IR absorption spectra of GST system are available for the frequency range of RS-spectrum, on which conclusions about the molecular mechanism of the phase transition in this system is based.

The IR absorption in solids can provide useful information about the lattice vibration density and structure of solids. The vibrations that contribute to IR absorption yield the most direct structural information because their frequencies are determined primarily by the nearest interactions, and thus, the relative IR activity are governed by local molecular symmetry. IR spectroscopy is one of the most frequently used spectroscopic tools for the study of the crystals and amorphous materials (including chalcogenide) [9]. Its application for studying the structure of short-range order and the dynamics of individual structural units of GST would be quite natural. This is especially so at low frequencies, where manifest multiphonon absorption in groups of the short-range order, lattice absorption in the crystal, and disorder-induced absorption in glasses ("boson peak" by terminology of RS-spectroscopy [10]) is manifested.

However, it is only known about the optical properties of the GST system that these materials have high transparency in the infrared range, from the electronic absorption edge up to the multiphonon edge near 20 micrometers. However, spectrophotometry has been recently used in the mid-IR region

50 to measure the transmittance of selected materials from this system [11]. The experimental data were  
51 successfully interpreted in terms of Drude-type plasma of free carriers and it was found that the main  
52 increase of optical constants occurs in the far-infrared domain. Consequently, the far-infrared  
53 spectroscopy appears to be convenient experimental method to study directly the structure and  
54 dynamics of the GST system. This is also evidenced by the results of the comparative study and  
55 analysis of the terahertz (THz) time-domain spectra of four different GST compounds, in whose  
56 spectra a phonon mode and a contribution of free charge carriers at range of 10-80  $\text{cm}^{-1}$  [12] are  
57 observed.

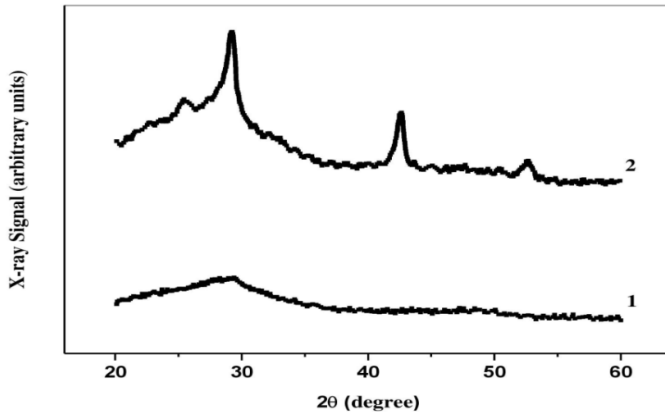
58 The aim of the present study was to obtain IR transmission spectra of polycrystalline and glassy  
59 material of a GST system containing 15 at % germanium, 15 at % antimony, and 70 at % tellurium  
60 (henceforth  $\text{Ge}_{15}\text{Sb}_{15}\text{Te}_{70}$ ) in the region 20-400  $\text{cm}^{-1}$ , to analyze these spectra on the basis of  
61 calculation and published data, and to find the relationship between the parameters of the far-IR  
62 spectra and the molecular characteristics of  $\text{Ge}_{15}\text{Sb}_{15}\text{Te}_{70}$ . The results are interpreted in terms of  
63 vibrations of isolated molecular units of the alloy under study. A detailed comparison of the spectra  
64 demonstrated that glassy  $\text{Ge}_{15}\text{Sb}_{15}\text{Te}_{70}$  exhibits characteristic extreme far-IR absorption as result of  
65 phonon coupling to modes which are not active in the corresponding crystalline material. The  
66 vibrational assignments of various absorption bands and the differences revealed in the spectra will  
67 make it possible to more confidently specify the possible molecular mechanism of the crystal-to-  
68 amorphous transition in GST alloys.

69

## 70 2. MATERIAL AND METHODS / EXPERIMENTAL DETAILS /

71

72 The melt-quench technique with elemental Ge, Sb and Te of 5N purity was used to  
73 prepare  $\text{Ge}_{15}\text{Sb}_{15}\text{Te}_{70}$  glassy samples [13]. The materials were weighed according to their atomic  
74 weight percentages and sealed in evacuated ( $\sim 10^{-3}$  Pa) quartz ampoules. The ampoules were kept in  
75 a furnace the temperature of which was raised up to 950  $^{\circ}\text{C}$  at a heating rate of 3-4  $^{\circ}\text{C min}^{-1}$ . The  
76 ampoules were frequently rocked for 20 h to make the melt homogeneous. Then the melts were  
77 rapidly quenched outside the furnace by dropping the ampoules in liquid nitrogen for fast cooling and  
78 to ensure the amorphization of the alloy. The alloys so obtained were crushed to the powder form for  
79 analysis. The nature of the thus prepared samples was confirmed by the X-ray diffraction patterns  
80 obtained with an Rigaku -D/MAX diffractometer with Cu  $K\alpha$  radiation ( $\lambda = 0.15406$  nm). Figure 1  
81 shows the XRD patterns for rapidly quenched and thermally annealed at 200  $^{\circ}\text{C}$  alloys. XRD pattern  
82 of rapidly quenched samples reveals the amorphous nature of the alloy as she do not show any  
83 spectacular peak while XRD pattern of samples annealed at 200  $^{\circ}\text{C}$  show the polycrystalline nature  
84 of the alloy.



85

86 Figure.1. X-ray diffraction spectra of GST alloy composition  $\text{Ge}_{15}\text{Sb}_{15}\text{Te}_{70}$ .  
87 1. X-ray scan of alloy quenched in liquid nitrogen.  
88 2. X-ray scan of thermally annealed alloy at 200 $^{\circ}\text{C}$ .  
89

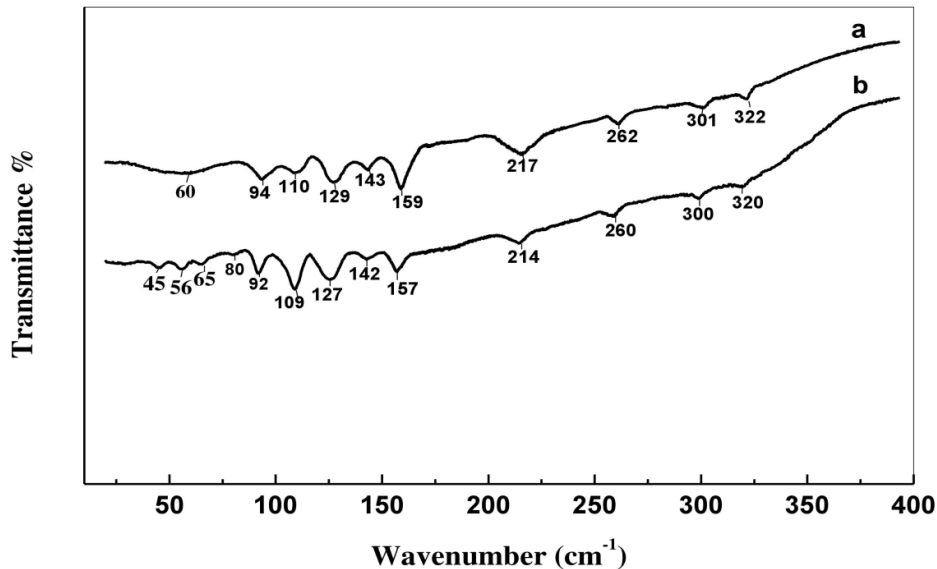
90 Bulk samples were characterized using energy dispersive X-ray spectroscopy (EDAX)(Zeiss EVO 40  
91 EP with EDAX attachment operated at 20 kV) for the analysis of compositions. EDAX results indicate

92 that the atomic percentages of  $\text{Ge}_{15}\text{Sb}_{15}\text{Te}_{70}$  compositions are close to starting elements (Ge-15.2,  
93 Sb- 15.1, Te - 70.3 at. %, with accuracy of  $\pm 5\%$ ). To obtain polycrystalline samples, the bulk samples  
94 were annealed in inert atmosphere for 120 min at temperature about  $20^\circ\text{C}$  above the temperature of  
95 amorphous - *fcc* phase transition determined by differential scanning calorimetry. Differential scanning  
96 calorimetry (DSC-50, Shimadzu) at heating rate of  $5^\circ\text{C}/\text{min}$  in a nitrogen flow was used to examine the  
97 thermal properties of investigated materials. Polycrystalline samples were crushed and pressed into  
98 Al pans. The temperature range studied was 20 to  $630^\circ\text{C}$ . The necessary amount of amorphous  
99 material (about 2–4 mg).

100 The far-IR absorption measurements were made in spectral range  $20\text{--}400\text{ cm}^{-1}$  at room temperature.  
101 Far-IR spectra were obtained on two spectrometers. A spectrometer designed at the Leningrad State  
102 University [14] and then modified with an OAP-7 and a new filtration system was used in the frequency  
103 range from 20 to  $150\text{ cm}^{-1}$ . The spectra in the range 150 to  $400\text{ cm}^{-1}$  were recorded with Hitachi FIS-  
104 21 (Japan) spectrometer. The resolution at a signal-to-noise ratio of the order of 100 was 1 to  $2\text{ cm}^{-1}$ .  
105 The peak positions of the spectral bands were determined to within 1 -  $2\text{ cm}^{-1}$ . All the measurements  
106 were made by using the polyethylene pellet method. The glassy and polycrystalline samples were  
107 thoroughly ground to an average size of 10-15  $\mu\text{m}$  in dry argon to preclude surface oxidation. The  
108 pellets were made by mixing 2-mg portion of a sample with 200 mg of spectroscopic grade  
109 polyethylene. The mixture was compacted into pellets with a hydraulic press ( $10\text{ tons cm}^{-2}$  for 5 min  
110 under vacuum). To take into account the absorption of polyethylene, it was used as reference. The  
111 spectrum of a sample was divided by the reference spectrum to eliminate the absorption of  
112 polyethylene.

### 114 3. RESULTS AND DISCUSSION

115  
116 The figure 2 shows the far-IR transmission spectra of polycrystalline and glassy GST material of  
117 composition  $\text{Ge}_{15}\text{Sb}_{15}\text{Te}_{70}$  in the region  $20 - 400\text{ cm}^{-1}$ . The recorded spectra have the form of an  
118 almost structureless plateau, with several peaks of the overlapping absorption bands seen on its  
119 background. The most distinct of these are the bands at  $\sim 60\text{ cm}^{-1}$ ,  $94\text{ cm}^{-1}$ ,  $110\text{ cm}^{-1}$ ,  $129\text{ cm}^{-1}$ ,  $159\text{ cm}^{-1}$ ,  
120  $217\text{ cm}^{-1}$ , and  $262\text{ cm}^{-1}$  in the spectrum of glassy and at  $45\text{ cm}^{-1}$ ,  $56\text{ cm}^{-1}$ ,  $65\text{ cm}^{-1}$ ,  $92\text{ cm}^{-1}$ ,  $109\text{ cm}^{-1}$ ,  $127\text{ cm}^{-1}$ ,  
121  $157\text{ cm}^{-1}$ , and  $214\text{ cm}^{-1}$  in the spectrum of polycrystalline material.



122

123 . Figure 2. Far-infrared spectra of GST system composition  $\text{Ge}_{15}\text{Sb}_{15}\text{Te}_{70}$  in the  
124 amorphous (a) and the crystalline (b) state.

125 These bands were tentatively assigned on the basis of calculations in which the GST alloy is regarded  
126 as a 3D polymer. Its structure was expressed in the form of the two covalently bound structural units:

127 tetrahedral “molecules” of germanium tetratelluride ( $\text{GeTe}_4$ ) in regions with a short-range order and  
 128 pyramidal “molecules” of antimony tritelluride  $\text{SbTe}_3$ . The validity of this approach follows from the  
 129 close relationship between the vibrational spectra of molecules or molecular ions and those of glass-  
 130 like solids containing the same or analogous structural groups in the form of regions with a short-range  
 131 order.

132 The  $\text{GeTe}_4$  molecule has 5 atoms and thus supports 15 modes of motion, including 3 pure rotations  
 133 and 3 pure translations. The  $T_d$  symmetry of the  $\text{GeTe}_4$  molecule leads to 6 zone-center modes  
 134 following the decomposition in standard notation [15]:

135  $\Gamma(T_d) = A_1 + E + F_1 + 3F_2$ ,

136 where  $F_1$  corresponds to a pure rotation (noted as R in the literature), and one of the  $F_2$  is a pure  
 137 translation (designated as T). R and T modes are related to the external modes. The modes derived  
 138 from the tetrahedral  $A_1$ , E and  $2F_2$  modes are usually named as  $v_1$ ,  $v_2$ ,  $v_3$  and  $v_4$ , respectively, and  
 139 are regarded as internal modes of the  $\text{GeTe}_4$  tetrahedra in  $\text{Ge}_{15}\text{Sb}_{15}\text{Te}_{70}$ .

140 The modes which predicts a group theory for a tetrahedral symmetry and the calculated phonon  
 141 frequencies at the  $\Gamma(T_d)$ -point are listed in Table 1. They are attributed as shown in Table 1 below in  
 142 accordance with the assignments of the germanium tetraiodide ( $\text{GeI}_4$ ) molecular vibrations [16, 17].  
 143

144 **Table 1. Normal vibrational modes of the  $\text{GeI}_4$  and  $\text{GeTe}_4$  tetrahedra.**

145 **From the spectrum of a Ge-Sb-Te alloy composition  $\text{Ge}_{15}\text{Sb}_{15}\text{Te}_{70}$ .**

Normal vibrational mode ( $\text{cm}^{-1}$ ) <sup>*</sup>						
substance	v1	v2	v3	v4	vR	vT
$\text{GeI}_4$	159	60	264	80	56 [19]	-
$\text{GeTe}_4$	125	87	209	78	60	55
$\text{Ge}_{15}\text{Sb}_{15}\text{Te}_{70}$	127	92	214	80	65	60

146 \*  $v_1$  and  $v_3$  – the stretching modes for symmetric and antisymmetric vibrations, respectively;  
 147  $v_2$  and  $v_4$  – bending modes for symmetric and antisymmetric vibrations, respectively;  
 148  $v_R$  and  $v_T$ - external modes for pure rotation and pure translation, respectively.

149 The analogy between the modes of the  $\text{GeTe}_4$  and the  $\text{GeI}_4$  tetrahedra can be used because the  
 150 mass ratio of germanium tetraiodide is very similar to germanium tetratelluride, and, therefore, a  
 151 correspondence in the respective frequencies can be expected.

152 Although only the  $v_3$  and  $v_4$  modes are IR-active in tetrahedral  $\text{GeX}_4$  molecules, it is expected that all  
 153 the fundamental modes appear in IR absorption spectra because of the violation of the selection rules  
 154 in polycrystalline and glassy materials. In addition, the structure of crystalline GST is only “rock salt  
 155 like” [1].

156 The  $\text{SbTe}_3$  molecule crystallizes in a structure with symmetry  $C_{3v}$ . There are four atoms per unit cell,  
 157 and, consequently,  $\text{SbTe}_3$  exhibits 12 phonon modes, including external R and T modes for each  
 158 wavevector K. A group-theoretical analysis yields for  $K = 0$  the following reduction:  $\Gamma_{\text{tot}}(C_{3v}) = 2A_{1g}$   
 159  $+ 2A_{1u} + 2E_g + 2E_u$ , which splits into acoustical modes and IR- or Raman-active optical modes as  
 160 follows:  $\Gamma_{\text{acoustical}} = A_{1u} + E_u$ ,  $\Gamma_{\text{Raman}} = 2A_{1g} + 2E_g$  and  $\Gamma_{\text{IR}} = A_{1u} + E_u$ , where one of the  $A_{1u}$  corresponds to a  
 161 pure rotation (designated as  $v_R$  here) and one of the  $E_u$  is a pure translation (designated as  $v_T$  here).  
 162 Following the spectroscopic notation, the stretching modes are designated by  $v_1$  and  $v_3$  for the totally  
 163 symmetric and the antisymmetric (double-degenerate) vibrations, respectively. Analogously, the  
 164 bending modes correspond to  $v_2$  ( $A_1$ ) and  $v_4$  (E). All four vibrations are both infrared- and Raman-  
 165 active.

166 The modes predicted by the group theory for a pyramidal symmetry and the calculated phonon  
 167 frequencies at the  $\Gamma_{\text{tot}}(C_{3v})$ -point are listed in Table 2. They are attributed as shown in Table 2 below

168 in accordance with the assignments of the of the antimony triiodide ( $\text{SbI}_3$ ) molecular vibrations [18].  
 169 The IR band assignments given here can be further substantiated by comparing the ratios between  
 170

171 **Table 2. Normal vibrational modes of the  $\text{SbI}_3$  and  $\text{SbTe}_3$  pyramids.**

172 **From the spectrum of a Ge-Sb-Te alloy composition  $\text{Ge}_{15}\text{Sb}_{15}\text{Te}_{70}$ .**

substance	Normal vibrational mode ( $\text{cm}^{-1}$ ) <sup>*</sup>						v3/v1	v4/v2
	v1	v2	v3	v4	vR	vT		
$\text{SbI}_3$	177	89	147	71	67,5	45,5	0.83	0.80
$\text{SbTe}_3$	164	122	145	106	53	46	0.88	0.86
$\text{Ge}_{15}\text{Sb}_{15}\text{Te}_{70}$	157	127	142	109	56	45	0.90	0.87

173 v1 and v3 – the stretching modes for symmetric and antisymmetric vibrations, respectively;  
 174 v2 and v4 – bending modes for symmetric and antisymmetric vibrations, respectively;  
 175 vR and vT- external modes for pure rotation and pure translation, respectively.  
 176

177 the experimental frequencies of the stretching modes (v3/v1) and of the bending (v4/v2) modes for  
 178  $\text{SbI}_3$  with similar values obtained in calculating the phonon modes for  $\text{SbTe}_3$ . The important aspect of  
 179 this comparison is that the frequency ratios v3/v1 and v4/v2 are essentially the same for the  $\text{SbI}_3$  and  
 180  $\text{SbTe}_3$ .

181 The calculated assignments of the IR bands in the spectrum of the crystalline  $\text{Ge}_{15}\text{Sb}_{15}\text{Te}_{70}$ ,  
 182 presented in the Tables 1 and 2 are qualitatively comparable with assignment of Raman frequencies  
 183 of GST materials, reported in literature [19, 20]. So, main Raman bands peaked at  $127\text{ cm}^{-1}$  and  $157$   
 184  $\text{ cm}^{-1}$  in cubic  $\text{Ge}_{22}\text{Sb}_{22}\text{Te}_{56}$  were also associated with stretching modes of  $\text{GeTe}_4$  tetrahedra and  
 185  $\text{SbTe}_3$  pyramids, respectively. The theoretical calculations made in the study show that bands peaked  
 186 at  $127\text{ cm}^{-1}$  and  $157\text{ cm}^{-1}$  have also a contribution of v2( $A_{1u}$ ) and v1( $E_u$ ) modes of  $\text{SbTe}_3$ , respectively.  
 187 The lower frequency band, covering  $85\text{--}115\text{ cm}^{-1}$  frequency region of the far-IR spectrum of  
 188  $\text{Ge}_{15}\text{Sb}_{15}\text{Te}_{70}$  is comparable in intensity with the peaks of stretching modes  $\text{GeTe}_4$  and  $\text{SbTe}_3$  and is  
 189 formed by at least two overlapping bands at  $92\text{ cm}^{-1}$  and  $110\text{ cm}^{-1}$ . According to the calculations, these  
 190 can be attributed to bending modes v2 (E) and v4 ( $E_u$ ) of the  $\text{GeTe}_4$  tetrahedra and  $\text{SbTe}_3$  pyramids,  
 191 respectively. In the frequency range  $180\text{--}330\text{ cm}^{-1}$ , at least four small bands peaked at  $\sim 214$ ,  $260$ ,  
 192  $300$ , and  $320\text{ cm}^{-1}$  can be distinguished in the far-IR spectrum of crystalline  $\text{Ge}_{15}\text{Sb}_{15}\text{Te}_{70}$  (see Figure  
 193 2). The first of these, lying at  $214\text{ cm}^{-1}$ , can apparently be assigned to v3 ( $F_2$ ) asymmetric stretching  
 194 modes of  $\text{GeTe}_4$  tetrahedra. An analogous feature was observed in Raman spectra of bulk crystalline  
 195  $\text{GeTe}$ , which are isostructural to  $\text{Ge}_{22}\text{Sb}_{22}\text{Te}_{56}$  [21]. The weak bands at  $260$  and  $320\text{ cm}^{-1}$  are quite  
 196 probably due to the so-called 2 - phonon vibrational absorption arising from excitations of fundamental  
 197 molecular stretching modes of  $\text{GeTe}_4$  (at  $127\text{ cm}^{-1}$ ) and  $\text{SbTe}_3$  (at  $157\text{ cm}^{-1}$ ), respectively; while  
 198 absorption band near  $300\text{ cm}^{-1}$  can be attributed to vibrations of Ge-Ge ethane-like clusters [22]. The  
 199 absorption bands at the frequencies  $95\text{ cm}^{-1}$  and  $143\text{ cm}^{-1}$ , which were assigned to the modes v2(E)  
 200 and v3(E) of the  $\text{GeTe}_4$  and  $\text{SbTe}_3$ , respectively, in the far-IR spectrum of the Te-rich  $\text{Ge}_{15}\text{Sb}_{15}\text{Te}_{70}$   
 201 might also contain the contribution of the fragments consisting only of tellurium atoms [23].

202 The proposed interpretation of the IR-spectrum of polycrystalline  $\text{Ge}_{15}\text{Sb}_{15}\text{Te}_{70}$  can be used for the  
 203 attribution of the absorption bands at  $\nu > 80\text{ cm}^{-1}$  of the IR-spectrum of the same alloy in amorphous  
 204 (glassy) state. This is so because experimental spectra of these states practically do not differ from  
 205 each other in range in which intramolecular modes of the structural units of  $\text{Ge}_{15}\text{Sb}_{15}\text{Te}_{70}$ , are  
 206 manifested, except for a negligible red shift and changes in the shape of bands in the IR-spectrum of  
 207 polycrystalline  $\text{Ge}_{15}\text{Sb}_{15}\text{Te}_{70}$  with respect to that of the amorphous state. Because, as a rule, the  
 208 crystalline phase is more ordered than the amorphous one, this fact shows unusual similarity of the  
 209 amorphous and crystalline structures  $\text{Ge}_{15}\text{Sb}_{15}\text{Te}_{70}$  of short range order and leads to an assumption

210 of rather similar degree of topological 'disordering' between these two forms. This means that the local  
211 structure of the building blocks (tetrahedra and pyramids) of  $\text{Ge}_{15}\text{Sb}_{15}\text{Te}_{70}$  remains basically  
212 unchanged upon the phase transition from the crystalline to the amorphous phase.

213 At the same time, an analysis of Figure 2 readily shows that the amorphous to crystal transition appears  
214 in the IR- spectra of  $\text{Ge}_{15}\text{Sb}_{15}\text{Te}_{70}$  as drastic changes at  $\nu < 80 \text{ cm}^{-1}$ , where the lattice absorption due  
215 to external librational and translational degrees of freedom of the structural units of crystal is  
216 manifested.

217 The presence of absorption peaks at 65, 56, and 45  $\text{cm}^{-1}$  (modes  $\nu_R(\text{F1})$ ,  $\nu_T(\text{F2})$  and  $\nu_T(\text{E})$ ,  
218 respectively) in the IR spectrum of polycrystalline  $\text{Ge}_{15}\text{Sb}_{15}\text{Te}_{70}$  is due, according to the calculations,  
219 to the manifestation of the intermolecular librations and translations of tetrahedra and pyramids as a  
220 whole. The IR spectrum of glassy  $\text{Ge}_{15}\text{Sb}_{15}\text{Te}_{70}$  contains in the same frequency range only a single  
221 abnormally broad band peaked at  $\sim 60 \text{ cm}^{-1}$ , which can be readily assigned as the well-known band  
222 ubiquitously present in amorphous solids, i.e., the boson peak.

223 Boson peak is attributed to the disorder-induced absorption, which is a manifestation of a low energy  
224 vibrational excitations emerging from cancellation of the selection rules in an amorphous medium. The  
225 peak observed in the low-frequency spectra of glasses appeared to correspond to the peaks  
226 observed at low frequencies in region of acoustic phonons of corresponding crystals [24]. Its  
227 appearance in the low-frequency spectra of glasses at the phase transition indicates that, in the  
228 absence of a long-range order, a system of coupled harmonic oscillators of crystal became a system  
229 of disoriented oscillators in which only limited (on a scale of medium-range order) correlation between  
230 the intermolecular vibrational motions is preserved [25]. So, the boson peak is occasionally assigned  
231 to cooperative orientational motion (librations) of several molecular groups [26, 27].

232 That is, when IR-spectra of polycrystalline and glassy materials are compared in range in which  
233 intramolecular modes of the structural units of  $\text{Ge}_{15}\text{Sb}_{15}\text{Te}_{70}$  are manifested, there is no evidence  
234 about the contrasting local structure between the amorphous and the crystalline phases, so the  
235 appearance of the boson peak at frequencies of intermolecular modes suggests that the medium-  
236 range crystalline order is also preserved in glassy  $\text{Ge}_{15}\text{Sb}_{15}\text{Te}_{70}$ . These data clearly reflect the local  
237 ordering of the atoms in the amorphous state which is similar to that in the crystalline  $\text{Ge}_{15}\text{Sb}_{15}\text{Te}_{70}$   
238 but lacks long-range ordering.

239 The spectral changes at low optical frequencies suggest the following scenario of a phase transition in  
240 the system  $\text{Ge}_{15}\text{Sb}_{15}\text{Te}_{70}$ . Local distortions inherent "tetrahedral" and "pyramidal" structural units of  
241 glassy  $\text{Ge}_{15}\text{Sb}_{15}\text{Te}_{70}$ , which facilitate the formation of Ge-Ge and Ge-Sb bonds [28], and also  
242 correlated torsional oscillations (librations) of these structures with a noticeable share of vacancy form  
243 medium-range (chain-like) order in the system. This is evidenced of this is the presence of the boson  
244 peak in the spectrum. For the transition to occur, such a system in a metastable ordered state not  
245 require a restructuring of local structures, but rather reorientation of existing clusters (the chains). In  
246 essence, the order-disorder transition is in this case a relaxation transition by the fast  $\beta$ -relaxation  
247 Johari-Goldstein mechanism [29]. Such a transition requires the minimum input of power and has a  
248 nanosecond relaxation time.

249

#### 250 4. CONCLUSION

251

252 In the present study the far-IR transmission spectra of polycrystalline and glassy materials of the GST  
253 system of composition  $\text{Ge}_{15}\text{Sb}_{15}\text{Te}_{70}$  were measured in the spectral range 20 - 400  $\text{cm}^{-1}$  at room  
254 temperature and also analyzed on the basis of theoretical calculation and of the literature data.  
255 Although the made vibrational assignments of various absorption bands given here could be  
256 considered as tentative and alternative interpretations may be proposed, these assignments and the  
257 revealed differences in the spectra allow suggest the following possible molecular mechanism for  
258 unusual amorphization- crystallization process in GST alloys.

259 According to the majority of existing models, the presence of the boson peak, as an indication of a  
260 medium-range order existing in the structure of glasses, in the low-frequency spectra is associated  
261 with the correlative orientational motion (librations) of fragments a crystalline structure of glass. These  
262 fragments of a crystalline structure can play the role of crystallization centers on the nanometer scale  
263 and their correlative librational vibrations can be viewed as precursors of phonons due to short-range  
264 ordering. Then according to this model, the recrystallization from the amorphous phase may be  
265 achieved easily by reorientation of the randomly oriented fragments of a crystalline structure back to  
266 the original well-aligned structure of the crystalline phase. We emphasize that in this case  
267 crystallization of GST does not involve relaxation of the complete covalent network but is more like the

268 so- called  $\beta$ -relaxation, where only fragments of the network relax. This process requires very small  
269 atomic displacements and hence can be extremely fast.  
270 The results, by the example of the composition  $\text{Ge}_{15}\text{Sb}_{15}\text{Te}_{70}$ , demonstrate, that the use of far-IR  
271 spectroscopy has a clear potential to characterize of the local atomic structure and dynamics of the  
272 GST alloys. Further studies on the new GST materials will give possibility to improve the parameters  
273 of the already developed memory elements and will provide additional information about the nature of  
274 the switching effect.

275  
276

## 277 REFERENCES

278

- 279 1. Kolobov AV, Tominaga J. Chalcogenides: Metastability and Phase Change Phenomena; Press:  
280 Springer-Verlag, Berlin; 2012.
- 281 2. Meinders ER, Mijiritskii AV, van Pieterse L, Wuttig M. Optical Data Storage Phase-Change Media  
282 and Recording; Philips Research Book Series, V. 4. Press: Springer- Verlag, Berlin; 2006.
- 283 3. Burr GF, Breitwisch MJ, Franceschini M. et al. Phase change memory technology. J. Vac. Sci.  
284 Technology B 2010; 28:223-262.
- 285 4. Kolobov AV, Fons P, Frenkel AI, Ankudinov AL, Tominaga J, and Uruga T. Understanding the  
286 phase-change mechanism of rewritable optical media. Nature Materials. 2004;3(10): 703-708.
- 287 5. Shportko K, Kremers S, Woda M, Lencer D, Robertson J. Wuttig M. Resonant  
288 bonding in crystalline phase-change materials. Nature Materials. 2008;7(8):653-658.
- 289 6. Wuttig M, Lusebrink D, Wamwangi D, Welnic W, Gilleben M, Dronskowski R. The role of vacancies  
290 and local distortions in the design of new phase-change materials. Nature Materials. 2007; 6(2):122-  
291 128.
- 292 7. Raty JY, Godlevsky V, Ghosez P, Bichara C, Gaspard JP, and Chelikowsky JR. Evidence of a  
293 Reentrant Peierls Distortion in Liquid GeTe. Phys. Rev. Lett. 2000; 85:1950 - 1953.
- 294 8. Cai YF, P. Zhou P, Lin YY, Tang TA, Chen LY, Li J et al. Nitrogen and Silicon Co-Doping of  
295  $\text{Ge}_2\text{Sb}_2\text{Te}_5$  Thin Films for Improving Phase Change Memory Performance. Chin. Phys. Lett. 2007;  
296 24(3):781 - 783.
- 297 9. Moller K, Rothschild W. Far Infrared Spectroscopy. Press: Wiley, New York; 1971.
- 298 10. Martin AJ, and Brenig W. Model for Brillouin Scattering in Amorphous Solids. Phys. Status Solidi B  
299 1974; 64(1):163-172.
- 300 11. Mendoza-Galvan A, and Gonzalez-Hernandez J. Drude-like behavior of Ge:Sb:Te alloys in the  
301 infrared. J. Appl. Physics. 2000; 87:760-765.
- 302 12. Kadlec F, Kadlec C, Kuzel P. Contrast in terahertz conductivity of phase-change materials. Solid  
303 State Communications. 2012;152(10):852-855.
- 304 13. Dzhurkov V, Fefelov S, Arsova, Nesheva D, and Kazakova L. Electrical conductivity and optical  
305 properties of tellurium-rich Ge-Sb-Te films. Journal of Physics: Conference Series. 2014;558:012046 -  
306 1 - 6.
- 307 14. Ryzhov VA, Tonkov MV. Technique of far-IR spectroscopy. In: Denisov GS (ed) Molecular  
308 spectroscopy; Press: University Press, Leningrad; 1973.
- 309 15. Herzberg G. Molecular Spectra and Molecular Structure. II. Infrared and Raman Spectra of  
310 Polyatomic Molecules; Press: D. Van Nostrand, London; 1945.
- 311 16. Stammreich H, Forneris Roberto, and Tavares Yara. Raman Spectra and Force Constants of  
312  $\text{GeI}_4$  and  $\text{SnI}_4$ . J. Chem. Phys. 1956;25:1278-1279.
- 313 17. Delwaulle ML. Mise en evidence par l'effet Raman de la formation de chlorobromiodures de  
314 germanium lorsqu'onmelange les tetrachlorure, tetrabromure et tetraiodure de germanium. C. R.  
315 Acad. Sci. 1954; 238:84-87.French.
- 316 18. Kiefer W. Raman-Spektreneines  $\text{AsJ}_3$ -Einkristalls und von  $\text{SbJ}_3$  - und  $\text{BiJ}_3$  - Kristallpulvern. Z.  
317 Naturforsch. 1970; 25a:1101-1107. Germany.
- 318 19. Nemecek P, Nazabal V, Moreac A, Gutwirth J, Bene L, Frumar M. Amorphous and crystallized Ge-  
319 Sb-Te thin films deposited by pulsed laser: Local structure using Raman scattering spectroscopy.  
320 Materials Chemistry and Physics.2012; 136:935-941.
- 321 20. Kozyukhin S, Veres M, Nguyen HP, Ingrams A, Kudoyarova V. Structural changes in doped  
322  $\text{Ge}_2\text{Sb}_2\text{Te}_5$  thin films studied by Raman spectroscopy. Physics Procedia.2013; 44:82- 90.
- 323 21. Upadhyay M, Murugavel S, Anbarasu M, and Ravindran TR. Structural study on amorphous and  
324 crystalline state of phase change material. J. Appl. Phys. 2011;110:083711 - 1 - 6.
- 325 22. Koblar J, Arlin B, Shau G, Porezag DV, and Pederson MR. Raman-active modes of a- $\text{GeSe}_2$  and  
326 a- $\text{GeS}_2$  : A first-principles study. Phys. Rev. B 1999; 60:R14985 - R14989.

- 327 23. Grosse, P. and Richter, W. Physics of Non-tetrahedrally Bonded Elements and Binary  
328 Compounds. In: Madelung O (ed) Landolt–Bornstein -Group III Condensed Matter; Press: Springer,  
329 Berlin; 1998.
- 330 24. Grigera TS, Martin-Mayor V, Parisi G. & Verrocchio P. Phonon interpretation of the 'boson peak' in  
331 supercooled liquids. Nature.2003; 422:289-292.
- 332 25. Johari GP. Molecular inertial effects in liquids: Poley absorption, collision-induced absorption, low-  
333 frequency Raman spectrum and Boson peaks. J. Non-Crystalline Solids. 2000; 307-310:114-127.
- 334 26. Bembenek SD, Laird BB. Instantaneous normal modes analysis of amorphous and supercooled  
335 silica. J. Chem. Phys. 2001; 114: 2340-2344.
- 336 27. Baran J, Davydova NA, Pietraszko A. Spectroscopic study of the formation of molecular glasses.  
337 J. Molec. Structure. 2005; 744-747:301-305.
- 338 28. Kolobov AV, Krbal M, Fons P, Tominaga J, Uruga T. Distortion-triggered loss of long-range order  
339 in solids with bonding energy hierarchy. Nature Chemistry.2011; 3:311 - 316.
- 340 29. Johari GP. Localized molecular motions of  $\beta$ -relaxation and its energy landscape.  
341 J. Non-Crystalline Solids. 2002; 307-310:317-325.